UNDERWATER STEREO IMAGE ENHANCEMENT USING A NEW PHYSICAL MODEL

Shijie Zhang[⋆] *Jing Zhang*[⋆] *Shuai Fang*[†] *Yang Cao*[⋆]

[⋆] Department of Automation, University of Science and Technology of China
[†] School of Computer and Information, Hefei University of Technology, China

ABSTRACT

Stereo image applications are becoming more and more prevalent. However, there has been little research on stereo image enhancement. In this paper, we address the challenging problem of underwater stereo image enhancement. A new underwater imaging model is proposed and it can better describe the degradation of underwater images including color distortion and contrast attenuation. In addition, a novel observation that the intensity of the water part within the image is mainly contributed by the scattering light is also proposed. Coupling the proposed model and prior together, the parameters of scattering light can be estimated. Then an iterative approach to process stereo matching and stereo image enhancement alternatively is presented, which can significantly improve the quality of the images and depth maps. The experimental results demonstrate that the proposed method can significantly enhance the image visibility and achieve better depth perception.

Index Terms— underwater, stereo enhancement

1. INTRODUCTION

Due to the development and maturation of stereo display technologies, the demand for improving the quality of stereo image is significantly increasing nowadays. In classical image processing approaches, the image quality is usually improved by enhancing the intensity, contrast and color vividness. In terms of stereo images, the enhancement of depth perception is an additional crucial task. It has been shown in [1] that the inter-correlation between the left and right viewpoint image should be taken into account to increase the depth perception.

Meanwhile, there is an ever growing interest in acquiring clear underwater images in areas such as monitoring sea life, assessing biological environments [2, 3], autonomous underwater robotics [4, 5, 6] and underwater archaeology [7]. Capturing clear underwater images is challenging due to the haze caused by light scattering by particles present in the water, and color distortion due to varying degrees of light attenuation for different wavelengths [8, 9, 10].

In this paper, we address the challenging problem of underwater stereo image enhancement. Our work aims at compensating for both light scattering and color change in the light transmission process. Furthermore, our work also focuses on improving the depth perception of stereo images.

Several algorithms that deal with underwater images have been proposed in the literature. Generally, such algorithms may be categorized into two main groups: image based and model based approaches [11]. Many image-based techniques have been proposed. For example, Bazeille et al. used successive steps including correct non-uniform illumination, noise suppression and color adjustment to reduce the underwater disturbances [12]. Ahlen et al. estimated a hyperspectral image, color corrected the hyperspectral image and transformed it back to RGB space. [13]. Cosmin Ancuti et al. used image fusion for underwater image enhancement [14, 15]. These approaches are usually simpler and faster than model-based methods. However, these methods have limited capability to recover visibility [16]. As for model-based methods, underwater optical properties are usually incorporated into this inverse problem. For example, Schechner et al. exploited the polarization effects in underwater scattering to compensate for visibility degradation [17]. John Y. Chiang and Y. Chen proposed a wavelength compensation and dehazing based algorithm in [18]. These methods are more compact, but they usually require some model parameters which are scarcely known in tables.

The above image enhancement algorithms can be directly applied to each view to produce an enhanced stereo image pair. However, these approach neglect the inter-correlation between the left and right images. Single frame-based image enhancement algorithms may generate much inconsistencies between the stereo image pair, leading to eyestrain and visual fatigue. A state of the art enhancement algorithm for underwater stereo images should take this inter-correlation into consideration. E. Nascimento et al. presented a method that considers the quality of the image and disparity map for recovery of the structure of the underwater scene [11]. The Human visual system (HVS) and binocular just-noticeable-difference (BJND) are further utilized to enhance stereo perception [19, 20].

This paper presents an approach based on a new physical model. Different from the traditional model [17], the proposed model takes into account the light attenuation along the vertical depth of the scene. Also, it can better demonstrate

This work was supported by NSFC (No.61175033).

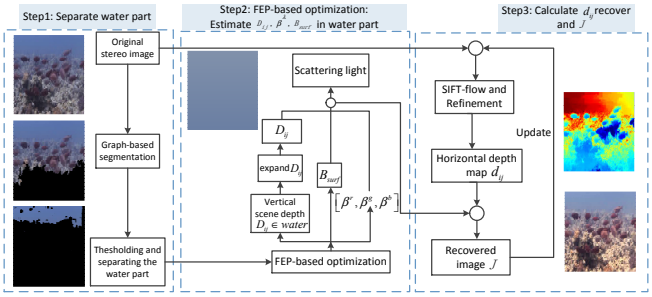

Fig. 1. Flowchart of our proposed method.

the underwater image degradation caused by light scattering an d attenuating. Moreover, this paper proposes a novel observation that the intensity of the water part within the image is caused mainly by the scattering light. Coupling the proposed model and prior together, the parameters of scattering light can be estimated by FEP-based optimization [21]. Then the inter-correlation inside the stereo image is utilized by processing stereo matching and image enhancement alternatively. Experiment results demonstrate that the proposed algorithm can significantly improve the quality of image and obtain better stereo perception.

2. FRAMEWORK

2.1. Proposed underwater Imaging Model

The degradation model used for bad weather is proposed to illustrate the formation of underwater images in some previous works [11]. However, the attenuation inconsistency of light with different wavelength traveling underwater is much greater than that in the air. For example, the attenuation for red light is much faster than for blue light while spreading underwater. An good underwater imaging model should consider the light attenuation along the horizontal depth from the object to the camera and the light attenuation along the vertical depth from the water surface to the object and camera. J. Y. Chiang and Y. Chen were the first to incorporate the former into the imaging model and propose a wavelength compensation algorithm [18]. In this paper, we further expand our analysis to include the attenuation of scattering light along the vertical path into the imaging model. The explicit form of the proposed model is as follows:

$$I_{ij}^{\lambda} = J_{ij}^{\lambda} \exp^{-\beta^{\lambda} D_{ij}} t_{ij}^{\lambda} + B_{surf} \exp^{-\beta^{\lambda} D_{ij}} (1 - t_{ij}^{\lambda}). \quad (1)$$

Here B_{surf} is the environmental light on water surface. ij is the pixel index, λ is the wavelength of light. I is the observed intensity and J is the scene radiance. D is the vertical scene depth. β^{λ} is the total attenuation coefficient of the environmental light.

2.2. Separating the water part

In this paper, we use a graph-based segmentation method [22] to separate the water part from the original under water image. However, there are usually objects (i.e., fish, coral) left in the water part, and we need to eliminate these outliers. Considering that the intensities of water part varies a little, we compute the variance of neighborhood pixels at each position, and then set a threshold to eliminate those pixels which have large variances. We set the threshold as 0.01-0.03.

2.3. FEP-based Optimization for the water part

We assume that the horizontal depth of water part is approximately infinite. So intensity of water part in the image is mainly contributed by the scattering light along the vertical path. According to the above assumption, the horizontal scene depth d_{ij} is so great as to be infinite, namely, the transmission $t_{ij}^{\lambda} \approx 0$. Consequently, a simplified model is presented for the water part:

$$I_{ij}^{\lambda} = B_{surf} \exp(-\beta^{\lambda} D_{ij}). \quad (2)$$

Therefore, $\{D_{ij}, \beta^{\lambda}, B_{surf}\}$ can be obtained by solving this optimization problem, which is formulated as:

$$\left\{D_{ij}^{*}, \beta^{\lambda *}, B_{surf}^{*}\right\} = \underset{\beta^{\lambda}, D_{ij}, B_{surf}}{\operatorname{argmin}} \sum_{\lambda \in \{r,g,b\}} \sum_{i,j} \left(\ln I_{ij}^{\lambda} - \ln B_{surf} + \beta^{\lambda} D_{ij}\right)^2 . \quad (3)$$

We divide the above optimization problem into the following three sub-problems where we solve D_{ij}, β^{λ} and B_{surf} alternately. The optimal solutions for D_{ij},β^{λ}, B_{surf} are as belows:

$$D_{ij}^{*} = \frac{\sum_{\lambda} (\ln B_{surf} - \ln I_{ij}^{\lambda}) \beta_{\lambda}}{\sum_{\lambda} (\beta^{\lambda})^2}. \quad (4)$$

$$\beta^{\lambda *} = \frac{\sum_{i,j} (\ln B_{surf} - \ln I_{ij}^{\lambda}) D_{ij}}{\sum_{i,j} (D_{ij})^2}, \quad (5)$$

$$B_{surf}^{*} = \exp\left(\frac{\sum_{\lambda} \sum_{i,j} \ln I_{ij}^{\lambda} + \beta^{\lambda} D_{ij}}{3|\Lambda|}\right). \quad (6)$$

However, since the optimal solutions of these three sub-problems may be not the global optimal solution of the original optimization problem, we apply Fast Evolutionary Programming algorithm (FEP) to choose the best result from a population of sub-optimal candidates [21]. In this paper, the Fitness function is defined as:

$$\mathrm{F} = \sum_{\lambda} \sum_{i,j} \left(I_{ij}^{\lambda} - B_{surf} \exp(-\beta^{\lambda} D_{ij})\right)^2. \quad (7)$$

2.4. Alternately calculate d and recover J

For the underwater stereo image, we calculate the horizontal depth map using a robust stereo matching algorithm, SIFT flow [23]. Then this initial horizontal depth d_0 is refined by applying a fast matting algorithm [24]:

$$d^* = \arg\min_d \lambda \|d - d_0\|^2 + d^T L d. \quad (8)$$

Once we get the horizontal depth d, we substitute it into Equation (1) along with the parameters of scattering light (B_{surf}, β^λ and D_{ij}), and recover the scene radiance J. Obviously, the left and right view share the same parameters of scattering light. Therefore, we use them and the depth map relative to right view to recover the right image. Considering that the recovered J are much clearer and share more distinct details, we can use them to recalculate the horizontal depth d. Consequently, we can calculate d and recover J alternately until obtaining stable results.

3. EXPERIMENT RESULTS

All the stereoscopic images are extracted from publicly available videos [25, 26]. The source code for the graph-based segmentation algorithm, SIFT flow and Laplacian matting are all available online. The minimum region in graph-based segmentation is set to 1/20 of the image size. The level for sift flow is set to 1 and the radius of matting is set to 9.

Table 1. The subjective experiment results.

	3D experience %				Contrast %				Color fidelity %			
	++	+	=	-	++	+	=	-	++	+	=	-
Red-cyan	10	80	10	0	40	50	10	0	0	10	90	0
Polarized	70	20	10	0	50	50	0	0	40	50	10	0
Red-cyan	0	80	20	0	40	60	0	0	0	10	80	10
Polarized	40	60	0	0	70	30	0	0	40	40	20	0
Red-cyan	0	50	40	10	40	40	10	10	0	50	30	20
Polarized	30	50	10	10	60	30	0	10	0	50	30	20
Red-cyan	0	50	50	0	30	70	0	0	0	30	70	0
Polarized	50	50	0	0	60	40	0	0	50	50	0	0

Since it is impossible to obtain a ground truth of enhanced underwater images, a user study is designed to test whether the enhanced results can deliver more pleasant 3D experience, more detail and more vivid color. The corresponding three criteria are 3D perception, contrast and color fidelity, respectively. Included, there are totally ten participants and four test stereo image pairs in total. Each participate would see two pairs of images in random order and then rate how good one is when compared with the other from the three criteria, respectively. Each participant was asked the following three questions: (1) Which stereo image is easier to perceive in 3D? (2) Which stereo image yields more detail? (3) Which stereo image shows more natural color? And four grades ("++","+","=","-", which means "significantly better","slightly better","almost the same", "slightly worse") are assigned. The images were observed with both red-cyan glasses and shuttered glasses. We calculated the statistics about how good the results were using the proposed method when compared with the original images. The statistical results are shown in Table 1. In terms of 3D experience, since low intensity and contrast will decrease viewers' stereo-perception acuity, most participants voted for the proposed method. For all four test cases, as high as 80% of the participants agreed that the proposed method yields more detail. Since red-cyan analyph images lose part of the color information when created, many participants give similar votes when viewing with red-cyan glasses. Additionally, when viewing the images with shuttered glasses, more than half of the participants considered the enhanced color to be more natural.

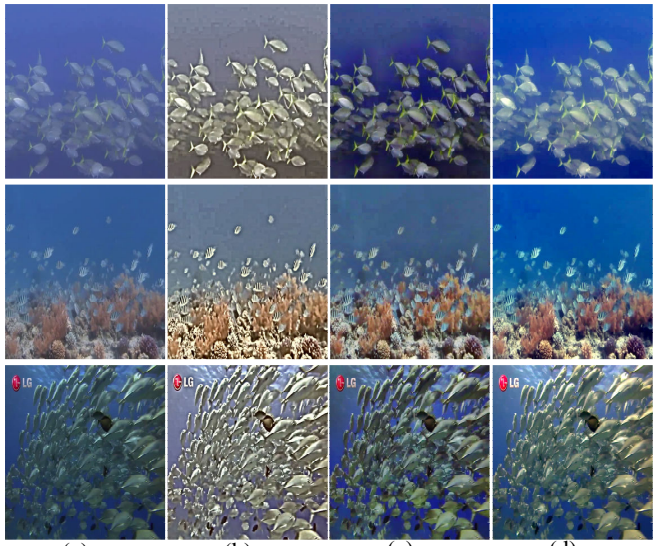

Fig. 2. (a) Left view of unprocessesd image. (b) Results by Bazeille[12]. (c) Results by fusion-based method [14]. (d) Our results. First image's $Nrer = [0.7457, 0.7790, 0.9521]$. Second image's $Nrer = [0.7933, 0.8155, 0.9014]$. Third image's $Nrer = [0.7949, 0.8299, 0.9258]$.

Next, in Figure 2, we compared our results with the methods in [12] and [14]. The three images are named shoal1, shoal2, shoal3, respectively. Results within each method [12] unveil the shadow of the input images but the results lack vivid colors. Method [14] aims at single underwater image enhancement. It achieves pleasant results for a single view, as shown in Figure 2 (c). In order to evaluate the enhancement algorithms' performance on the alleviation of the increase in the interdifference, the pixel matching error between two corresponding positions in the stereo image is computed according to the method used in [27]. By comparing the match-

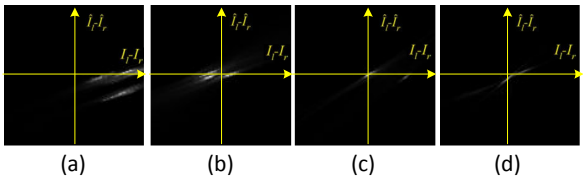

Fig. 3. Pixel matching error before and after enhancement processing (a)(b)Error curve between the original and enhanced images by [14] for shoal1 and shoal2 (c)(d)Error curve between the original and enhanced images by the proposed method for shoal1 and shoal2.

ing error before and after the enhancement, the increase in the interdifference can be evaluated. The distributions of the matching error values for shoal1 and shoal2 are demonstrated in Figure 3.The distributions of the matching error values are highly concentrated on the origin due to large smooth areas in the image. However, as shown in Figure 3 (a) and (c), the magnitudes of the error values tend to be increased by [14].This unnecessary increase in the interdifference could result in visible artifacts. The distributions in Figure 3 are more strongly concentrated at the origin, and the shape of the distribution is close to a line with a slope equal to 1.

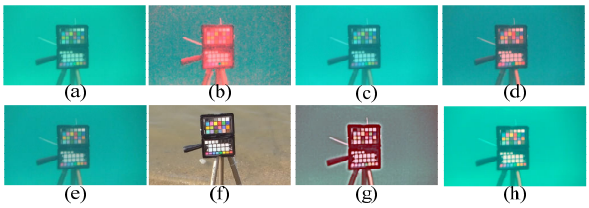

Fig. 4. (a) Left view of underwater color checker. (b)-(e) Results of Grey world, Grey edge, Grey shade and Max-rgb. (f) Color checker on the land. (g) Results of Bazeille[12]. (h) Results of our model.

Table 2. Color fidelity experiment of different methods.

Origin	GW	GE	GS	Max	[12]	Ours
18.85	19.05	18.63	20.59	20.13	18.94	19.51

To further evaluate the fidelity of the enhanced color, we took pictures for the X-Rite's Color Checker Passport underwater. The results are compared with several classical color constancy algorithms [28](Grey World, Grey Edge, Gray Shades and Max-rgb) and method of Bazeille [12], as shown in Figure 4. Since Passport's true color is known, we calculated each algorithm's PSNR values as a quantitative standard, as shown in Table 2. Here our result's PSNR ranks the third. However, the results by max-RGB are slightly dark, and the results by Gray Shades are a little reddish. Our result is more colorful and visually pleasing.

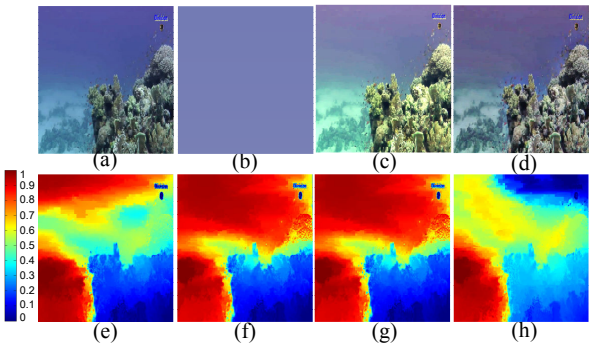

Fig. 5. Stereo geometry consistency comparison. (a) Left view. (b) Estimated results of scattering light. (c) Enhanced results of the left view after two iterations. (d) Enhanced results of fusion-based method [15]. (e)(f)(g) Obtained depth map for left image after zero/one/two iterations, respectively. (h) Obtained depth map by fusion-based method [15]. $Nrer = [0.8115, 0.8473, 0.9441]$.

Last, the proposed algorithm can provide a better depth perception than previous methods. After obtaining all model parameters, our algorithm will estimate horizontal depth d and enhanced J iteratively. Figure 5(e)(f)(g) shows the depth after zero/one/two iterations. As can be seen, the quality of depth maps is gradually becoming better. For example, the water part is becoming more homogeneous. The final obtained depth map is much more accurate than method [14].

4. CONCLUSION

In this paper, we have proposed an approach for the image enhancement of underwater stereo images based on a new physical model. To the best of our knowledge, our proposed model is the first to consider the attenuation of scattering light along the vertical path. Consequently, this model can more accurately illustrate the optical properties of underwater imaging. In addition, we have proposed an iterative algorithm to process the stereo matching and image enhancement alternately. This iterative process takes full advantage of the inter-correlation of the stereo image pair, leading to better 3D perception. Subjective and quantitative performance evaluation results have demonstrated that the proposed algorithm can significantly improve the quality of image and stereo perception.

Our work shares the common limitation of most model-based enhancement methods; the underwater imaging model may be invalid in some cases. For example, if there is an artificial light source, or the light propagation is inhomogeneous, more advanced models should be used to demonstrate these complicated phenomena.

5. REFERENCES

[1] Ian P. Howard and Brian J. Rogers, *Perceiving in Depth*, New York: Oxford University Press, 2012.

[2] S. Negahdaripour and C. Yu, *Underwater Robotic vehicles: Design and Control*, TSI Press, 1995.

[3] A. Trucco and V. Murino, "Guest editors introduction : Special issue on underwater computer vision and pattern recognition," *Comput. Vis. Image Underst.*, vol. 79, no. 1, 2000.

[4] M. Chyba, N. E. Leonard, and E. D. Sontag, "Optimality for underwater vehicles," in *Proc. IEEE Conf. on Decision and Control*, 2001.

[5] M. Purcell, C. von Alt, B. Allen, T. Austin, N. Forrester, R. Goldsborough, and R. Stokey, "New capabilities of the remus autonomous underwater vehicle," in *Proc. MTS/IEEE Oceans00, Providence, RI*, 2000, vol. 1, p. 147C151.

[6] C. Woosey and N. E. Leonard, "Moving mass control for underwater vehicles," in *Proc. American Control Conference*, 2002, p. 2824C2829.

[7] Y. Kahanov and J. Royal, "Analysis of hull reamins of the dor d vessel, tantura lagoon, israel," *Int. J. Nautical Archeology*, p. 257C265, 2001.

[8] J. R. Zaneveld and W. Pegau, "Robust underwater visibility parameter," *Opt. Exp.*, vol. 11, no. 23, pp. 2997C3009, 2003.

[9] E. Trucco and A. Olmos, "Self-tuning underwater image restoration," *IEEE Journal of Oceanic Engineering*, vol. 31, pp. 511–519, 2006.

[10] J. S. Jaffe, "Computer modeling and the design of optimal underwater imaging systems," *IEEE J. Ocean. Eng.*, vol. 15, no. 2, pp. 101C111, 1990.

[11] Erickson Nascimento and Mario Campos, "Stereo based structure recovery of underwater scenes from automatically restored images," in *Brazilian Symposium on Computer Graphics and Image Processing*, 2009.

[12] S. Bazeille, L. J. I. Quidu, and J. P. Malkasse, "Automatic underwater image pre-processing," in *In Proc. CMM*, 2006.

[13] J. Ahlen, D. Sundgren, and E. Bengtsson, "Application of underwater hyperspectral data for color correction purposes," *IEEE Trans. on Pattern Anal. Mach. Intell. (TPAMI)*, vol. 17, pp. 170–173, 2007.

[14] C. O. Ancuti, C. Ancuti, T. Haber, and P. Bekaert, "Fusion-based restoration of the underwater images," in *In Proc. ICIP*, 2011.

[15] C. O. Ancuti, C. Ancuti, T. Haber, and P. Bekaert, "Enhancing underwater image and videos by fusion," in *In Proc. CVPR*, 2012.

[16] Y.Y. Schechner and N. Karpel, "Clear underwater vision," in *in Proc. IEEE CVPR*, 2004.

[17] Y.Y. Schechner and Y. Averbuch, "Regularized image recovery in scattering media," *IEEE Trans. on Pattern Anal. Mach. Intell. (TPAMI)*, vol. 29, pp. 1655–1660, 2007.

[18] J. Y. Chiang and Y. Chen, "Underwater image enhancement by wavelength compensation and dehazing," *IEEE Trans. on Image Proc (TIP)*, vol. 21, pp. 1756–1769, 2012.

[19] M. M. Subedar and L. J. Karam, "Increased depth perception with sharpness enhancement for stereo video," *Proc. SPIE*, vol. 7524, pp. 1B, 2010.

[20] Y. Zhao, Z. Chen, C. Zhu, Y.-P. Tan, and L. Yu, "Binocular just-noticeable-difference model for stereoscopic images," *IEEE Signal Process. Lett.*, vol. 18, no. 1, pp. 19C22, 2011.

[21] X. Yao and Y. Liu, "Fast evolutionary programming," in *in Proc. Evolutionary Programming*, 1996.

[22] P. F. Felzenszwalb and D. P. Huttenlocher, "Efficient graph-based image segmentation," *International Journal of Computer Vision (IJCV)*, vol. 59, no. 2, pp. 167–181, 2004.

[23] Ce Liu, Jenny Yuen, and Antonio Torralba, "Sift flow: Dense correspondence across scenes and its applications," *IEEE Transactions on Pattern Analysis and Machine Intelligence*, vol. 33, no. 5, pp. 978– 994, 2011.

[24] A. Levin, "A closed-form solution to natural image matting," *IEEE Transactions on Pattern Analysis and Machine Intelligence*, vol. 30, no. 2, pp. 228–242, 2008.

[25] Tauchen Rotes Meer 3D, ," http://www.youtube.com/watch?v=MpmizLF4UhI.

[26] Tauchen im Roten Meer Part 2 3D, ," http://www.youtube.com/watch?v=TXpKdtcT_Vo.

[27] Seung-Won Jung, Jae-Yun Jeong, and Sung-Jea Ko, "Sharpness enhancement of stereo images using binocular just-noticeable difference," *IEEE Transactions on Image Processing*, vol. 21, no. 3, 2012.

[28] J.V.D. Weijer, T. Gevers, and A. Gijsenij, "Edge-based color constancy," *IEEE Trans. on Image Proc (TIP)*, vol. 16, pp. 2207–2214, 2007.